Structural Characterization of Lactate Dehydrogenase Dissociation under High Pressure Studied by Synchrotron High-Pressure Small-Angle X-ray Scattering[†]

Tetsuro Fujisawa,*[,‡] Minoru Kato,[§] and Yoji Inoko[||]

Structural Biophysics Laboratory, Harima Institute, The Institute of Physical and Chemical Research (RIKEN), SPring-8, Mihara, Mikazuki, Sayo, Hyogo 679-5143, Japan, Department of Chemistry, Faculty of Science and Engineering, Ritsumeikan University, 1-1-1 Noji-Higashi, Kusatsu, Shiga 525-8577, Japan, and Division of Biophysical Engineering, Graduate School of Engineering Science, Osaka University, Machikane-yama, Toyonaka 560-8531, Japan

Received October 27, 1998; Revised Manuscript Received February 9, 1999

ABSTRACT: The effect of high pressure on lactate dehydrogenase (LDH) was studied using small-angle X-ray scattering (SAXS). The SAXS results are interpreted in terms of the dissociation and association of LDH within a compression and decompression cycle and its temperature dependence. LDH consists of four identical subunits. At 120 MPa and 25 °C, 50% of the LDH dissociates into subunits, while at 10 °C, this occurs at 78 MPa. The hysteresis in the dissociation and association under pressure was confirmed in terms of the radius of gyration and was seen to be more conspicuous at low temperature. Forward scattering, $I(0)/C$, which is proportional to molecular weight, showed that LDH dissociated into dimer (not monomer) subunits under pressure. The application of high pressure to dissociated dimers induced irreversible aggregation. This result is in sharp contrast with the result of fluorescence spectroscopy suggesting a dissociated monomer [King, L., and Weber, G. (1986) *Biochemistry 25*, 3637−3640]. As for structural change after reassociation, there was little structural difference between native and drifted LDH. The difference was smaller than the structure change by ligand binding. At 200 MPa, the presence of five scattering peaks in the medium-angle region indicates that the dissociated dimer does not have a molten globule-like structure but a core structure. We propose a model of the dissociated dimer, based on the SAXS profile, in which the volume is reduced without disrupting the core structure.

The effects of temperature and chemical composition on protein stability have been thoroughly investigated; however, the effects of pressure have only been studied recently, and there have been relatively few studies in this area. Several reviews of the effects of pressure on proteins revealed that many single-chain monomeric proteins do not unfold at pressures below 500 MPa (*1*−*5*). In contrast, pressure-induced dissociation of oligomeric and multimeric proteins is observed below 200 MPa, where life in the deep sea is relevant. The effects of high pressure on oligomeric proteins, therefore, have been discussed as a possible mechanism underlying the growth inhibition of microorganisms at high pressures (*1*, *3*). Detailed studies on subunit−subunit and protein−nucleotide interactions have been done at high pressure (*4*, *6*).

One example, lactate dehydrogenase (LDH),[1] which consists of four subunits, has been extensively studied. The dissociation/inactivation of LDH under high pressure was studied by Jaenicke and co-workers (*2*). They showed the chemical equilibrium according to

{applying pressure}

native tetramer structure ⇔ 4(inactive monomer) ⇔ 4(partially unfolded monomer)

Observed deactivation paralleling subunit dissociation has been demonstrated by hybridization and chemical cross-linking. Weber and co-workers introduced fluorescence intensity measurement together with activity measurement in order to reveal conformational properties (*7*, *8*). They reported hysteresis phenomena: in dissociation under pressure, loss of activity occurs in parallel with dissociation, while during association by decompression, the time courses of spectral change and regain of activity differ. Upon release of pressure, the monomer associates immediately into a weak aggregate with a volume of the original tetramer but with diminished catalytic activity. Additionally, intermediate degrees of dissociation are observed when the pressure is increased to 200 MPa and lowered toward atmospheric pressure. The hysteresis effects are explained by a very slow reverse structural drift back to the native state proceeding only from the fully oligomeric form, "conformational drift":

{reduction of pressure}

dissociated monomer ⟹ modified (drifted) tetramer ⇔ native structure

conformational drift

They showed that "equilibrium" dissociation constants depend on concentration and differ from the ratio between

[†] This work was in part supported by a Grant-in-Aid for Scientific Research from the Japanese Ministry of Education, Science and Culture. These SAXS measurements were performed with the approval of the Program Advisory Committee of the Photon Factory (proposal nos. 93-G034, 93-G038, 95G086, and 95G092).

* Corresponding author.

[‡] The Institute of Physical and Chemical Research.

[§] Ritsumeikan University.

[||] Osaka University.

[1] Abbreviations: LDH, lactate dehydrogenase; SAXS, small-angle X-ray scattering; R_g, radius of gyration.

10.1021/bi982558d CCC: $18.00
Published on Web 04/30/1999

forward and backward rates. Separation of the subunits may be deemed complete in 1 ns, while subsequent changes in conformation proceed of a rate of 10^6 mol^{-1} s^{-1}. The origin of dissociation is thermodynamically attributed to protein−protein bonds that undergo the largest repulsion force when the distances between atoms decrease on application of pressure (*4*).

Two important findings in relation to "conformational drift" theory have been reported: first, high pressure modifies the structure of native molecules and early products of dissociation (*9*, *10*), a finding that disagrees with the important assumption of the analysis of dissociation equilibrium; and secondary, the aggregation product of oligomeric protein made by high pressure can be reversely folded into native structure (*11*). Aggregation might participate in hysteresis phenomena.

There are two main issues discussed in this paper. The first is structural characterization of the hysteresis phenomena and their dissociation products. We present different models of pressure-induced dissociation of LDH. The second issue is the structural interconversion between the modified (drifted) tetramer and native tetramer. At atmospheric pressure, there are many indications that hydrodynamic volume decreases upon binding ligand. In the presence of a ligand at the nonsaturating concentration, pressure shifts the equilibrium toward a holoenzyme, and the holoenzyme dissociates only after full saturation at a limiting pressure (*3*). One of the reasons why we chose to study LDH as an example of oligomer dissociation was that at atmospheric pressure apo- and holo-LDH undergo a large structural change, including displacement of the four subunits (*12*). Even in the absence of ligands, drifted apo-LDH may take on a configuration similar to that of holoenzyme because of its decreased volume. We describe the differences between drifted, native apo- and holo-LDH. Finally, we discuss the interpretation of the hysteresis effect in terms of the SAXS results.

Measurement of high-pressure SAXS is very useful for understanding the effects of pressure in biology. As one can see from Le Chatlier's principle, which states that at equilibrium a system tends to minimize the effect of any external factor by which it is perturbed, an increase in pressure reduces the volume of a system and consequently changes SAXS. SAXS capable of detecting volume change accurately should be an essential tool for studying pressure effect on proteins. However, there have been few high-pressure studies using SAXS from protein solutions because of the experimental difficulty. There have been two major problems: The first problem is the large absorption and parasitic scattering from the cell window material, and the other is that it is very difficult to have identical conditions when measuring sample and buffer solutions. This is because application of pressure often changes the sample thickness irreversibly and destroys the parallelism of the two windows. This difficulty has been overcome by a combination of two techniques: intense synchrotron X-ray source and hydrostatic high-pressure cells with diamond windows (*13*−*16*). The use of hydrostatic cells enabled us to perform quantitative measurements under high pressure (*16*).

EXPERIMENTAL PROCEDURES

Sample Preparations. Pig heart lactate dehydrogenase was purchased from Boehringer Mannheim. The protein was passed through a desalting column, P6-DG (Bio-Rad), in order to replace buffer media as well as to remove small particles. The buffer was 50 mM Tris-HCl, pH 7.5, 1 mM EDTA, and 1 mM DTT containing 8% glycerol. The protein concentration was determined spectrophotometrically using $A_{280}^{1\%} = 14.9$.

Static SAXS Experiment. All SAXS experiments were performed at beamline 10C at Photon Factory, Tsukuba, Japan (*17*). With a fix-exit double-crystal monochromator Si(111), the X-ray wavelength was tuned to 1.488 Å. Measurement of ligand-induced structural change of LDH at ambient pressure was done in a buffer containing 100 mM potassium-phosphate (pH 7.0), 1 mM EDTA, and 0.1 mM DTT in the presence or absence of 10 mM NAD. A series of different concentrations (1−7 mg/mL) were used to eliminate interparticle interference. Two camera lengths, 80 and 200 cm, were used. The data collection time was 600 s.

High-Pressure SAXS Experiment. The detailed structure of a high-pressure cell is described elsewhere (*17*). The beam size was reduced to 1.2 mm × 1.2 mm by guard slits. The wavelength was decreased to 1.3 Å, which was the shortest wavelength available at the beamline. The SAXS profile was recorded by a one-dimensional position-sensitive proportional counter (PSPC) with a 10-mm slit. The incident X-ray intensity was scaled by an ion chamber current installed before the sample cell. The distance between the sample position and the detector was 55 cm. The X-ray absorption was measured by direct beam intensity attenuated by 1.3 mm Al foil at each pressure. In high-pressure experiments, a series of measurements where transmission between the solution and buffer differed were rejected. From the definition of scattering intensity, scattering from proteins should always be positive, which means that a raw sample profile is always larger than that of the buffer in all scattering regions. The results of a series of experiments in which the buffer profile was larger than that of the sample in some regions were also rejected. The temperature of the cell was maintained at a constant level by circulating temperature-controlled water in a cell jacket. After changing the pressure, we waited for at least 5 min to equilibrate the temperature. The data collection time was 900 s. No radiation damage was detected during compression and decompression cycles.

Data Analysis of SAXS Profiles. Subtraction of the buffer profile, absorption correction, and the analysis described below were all performed using a personal computer (NEC PC9800) (*18*). The radius of gyration, R_g, was determined from the linear region of the $\ln[I(S)]$ vs S^2 plot, the so-called Guinier plot, where $S = 2\sin\theta/\lambda$, 2θ is the scattering angle, λ is the wavelength, and $I(S)$ is the scattering intensity at S. The distance distribution function, $P(r)$, which is calculated from the Fourier transform of $I(S)$, indicates the distribution of the interatomic vector of a given length of a molecule. This was calculated by both Moore's algorithm (*19*) and the GNOM package (*20*). Intensity functions from atomic coordinates were calculated using Debye's formula (*21*):

$$I(S) = \sum\sum f_i f_j \{\sin(2\pi S r_{ij})/(2\pi S r_{ij})\}$$

where f_i, f_j are structure factors of the ith and jth atom, respectively; and r_{ij} is the distance between the ith and jth atom.

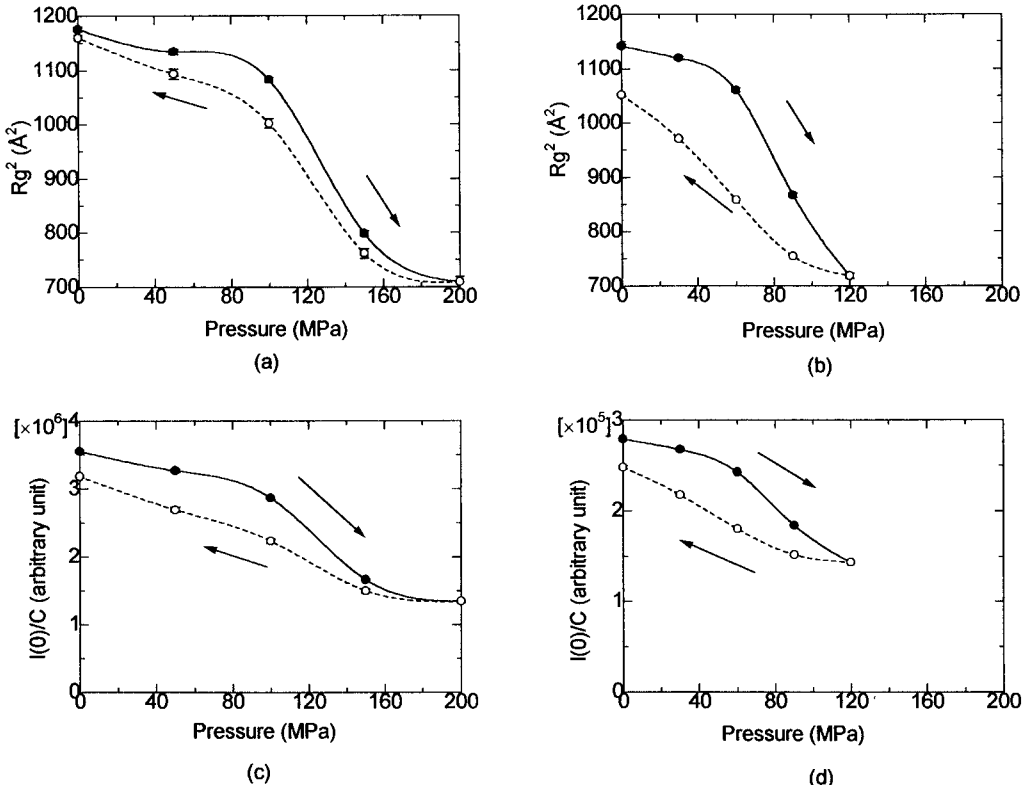

FIGURE 1: R_g change of LDH according to pressures of LDH at 25 °C (a) and at 10 °C (b). $I(0)/C$ change according to pressures of LDH at 25 °C (c) and at 10 °C (d). Protein concentrations are 16.3 and 20 mg/mL at 25 and 10 °C, respectively. Compression (solid line) and decompression (broken line) are drawn separately. Further compression beyond 200 and 120 MPa resulted in protein precipitation at 25 and 10 °C, respectively. The fitted region used for R_g determination was 60×10^{-6} Å$^{-2} < S^2 < 200 \times 10^{-6}$ Å^{-2}.

This equation does not take into account exclusion volume and hydration shell, and therefore only a qualitative comparison between crystal and solution structures is possible.

The R_g of the model structure was calculated using the CRYSOL program package (*22*). CRYSOL is a program for evaluating solution scattering with the hydration shell from atomic coordinates by approximating an envelope particle with a spherical harmonic function. The hydration shell width was taken as 3 Å, and the maximum harmonics number was 12. The surface area and volume were calculated with Voronoi polyhedra by Gerstein's surface and volume calculation program library (*23*, *24*). The first derivative of $I(S)$ is given by

$$dI(S)/dS = (I(S)_{I+1} - I(S)_I)/\Delta S$$

where $I(S)_I$ is the intensity of ith channel and ΔS is the increment of S per channel. Before calculation of $dI(S)/dS$, $I(S)$ was smoothed with the cubic spline function.

RESULTS

Subunit Dissociation upon Compression Observed by SAXS. Here, we describe the change in overall structure and molecular weight upon application of a compression and decompression cycle. R_g is more sensitive to subunit configuration than Stokes' radius; R_g is the second momentum of excess electron distribution, while Stokes' radius is the function of shape only. $I(0)/C$ is the scattering intensity at 0° divided by the weight concentration C (mg/mL) of protein and is proportional to molecular weight. Figure 1 shows changes in R_g and $I(0)/C$ upon application of a compression and decompression cycle of LDH (16.3 mg/mL at 25 °C and 20 mg/mL at 10 °C, respectively). Below 60 MPa at 25 °C or 40 MPa at 10 °C, both R_g and $I(0)/C$ were decreased slightly. This small decrease can be interpreted as elastic change in the native tetramer, which includes the loss of hydration. In these pressure regions, the majority of LDH seems to remain as the native tetramer. When R_g and $I(0)/C$ started to decrease over 40−60 MPa, they changed simultaneously. Since these two values are ensemble averages of a given system, the change in R_g reflects the equilibrium shift from native tetramer to dissociation. The dissociation critical pressures were estimated from apparent R_g^2 to be 120 MPa (Figure 1a) and 78 MPa (Figure 1b) at 25 and 10 °C, respectively. A destabilizing effect due to reduction in temperature was also seen in SAXS. Lowering the temperature shifted the midpoint to −42 MPa in terms of overall structure, which is comparable with fluorescence data.

Protein Concentration Dependency on Subunit Dissociation. Weber reported that dissociation phenomena are dependent on protein concentration (*7*). The protein concentration (about 140 nM) used for SAXS is about 50 times higher than that of fluorescence (only a few nanomolar). The critical pressure of fluorescence (∼145 MPa at 25 °C) is, however, compatible with that of SAXS, where a pressure shift of +56 MPa was expected (*7*). The critical pressure of the protein concentration range of SAXS (5.6, 16.3, and 40 mg/mL at 25 °C) lay within ±3 MPa, where a pressure shift of 30 MPa was expected.

Number of Subunits of Dissociated Products. The most important finding from this study concerns the dissociation number. The effect of pressure on $I(0)/C$, i.e., molecular weight, is shown in Figure 1c,d. The value of $I(0)/C$

Table 1: Radii of Gyration at Different States of LDH

state of LDH	apparent R_g (Å)
atmospheric pressure	34.3 ± 0.1
apo	34.6 ± 0.1[a]
holo	33.8 ± 0.2[a]
200 Mpa	26.6 ± 0.4
reconstituted LDH at atmospheric pressure	34.1 ± 0.1

[a] These values are R_g at infinite dilute solution measured by a static cell.

Table 2: Structural Parameters of Models

	R_g (Å)	volume (Å^3)	surface area (Å^2)
whole protein	32.43	224 480	42 130
model (a)	30.17	105 750	26 210
model (b)	28.28	105 720	24 230
model (c)	29.48	105 650	28 140
monomer	22.51	48 050	11 150

decreased to 51% and 38% from the initial state at 10 and 25 °C, respectively, clearly indicating that the dissociation proceeded not to a monomer but to a dimer. This is also consistent with the fact that 26.6 Å of R_g at 200 MPa is much larger than 22.5 Å of that expected for a monomer (Tables 1 and 2). The application of further pressure resulted in irreversible aggregation. The dissociated dimer is completely different from other observations by fluorescence spectroscopy (*3*, *7*). One possible explanation is the presence of glycerol, which is known to induce preferential hydration of the protein−water interface (*25*) and is known to reduce conformational drift owing to a more limited interaction with water. It should also be considered that the degrees of dissociation calculated by fluorescence result in serious error if the polarization values differ between native and dissociated products.

Hysteresis Effect Observed by SAXS. The recoveries of R_g and $I(0)/C$ upon decompression were similar, indicating that there was an equilibrium shift from dissociated subunits to a tetramer. Hysteresis was evident irrespective of temperature, though tetramerization was incomplete at 10 °C, while at 25 °C the recovery was completed. One compression and decompression cycle takes roughly 3 h, and therefore association proceeds at a constant rate of about 10^{10} mol^{-1} s^{-1} at 5 °C. At 25 °C, hysteresis pressures were 20 and 10 MPa for fluorescence and SAXS, respectively. At 10 °C, the delay in recovery appears to be more conspicuous compared to reported spectroscopy. SAXS needs a longer measurement time compared to spectroscopy, so that dissociated products remain for a longer time under high pressure. The difference in measurement time may contribute to the slower recovery after decompression in SAXS, because a long exposure to high pressure is known to slow the recovery of activity. It should be noted that the transition rate of overall dimensions becomes slower than that of local structure under high pressure in the case of pressure denaturation of a small monomeric protein (*15*), which may occur in association and dissociation phenomena.

Subunit Rearrangement after Reassociation. We were interested in the difference in structure before and after compression in terms of subunit displacement. An oligomeric protein is thought to exist in two main conformations, T and R, determined by the disposition of the subunits (*26*). In crystal apo and holo states, LDH has very similar R_g values (*27*, *28*), while clear compaction of the molecule was

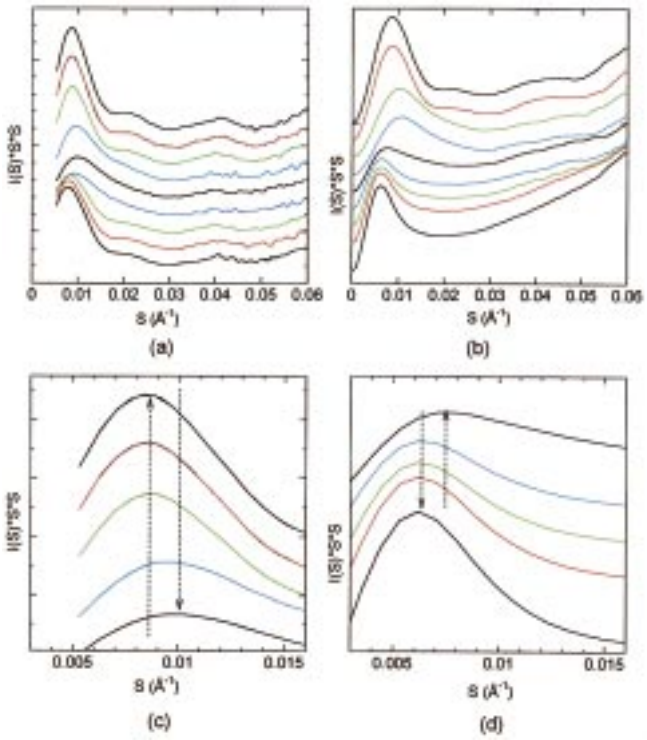

FIGURE 2: (a) Kratky plot of LDH at 25 °C. Protein concentration was 40 mg/mL. From the top: 0.1, 50, 100, 150, 200, 150, 100, 50, and 0.1 MPa. Each plot has been shifted so it can be seen clearly. (b) Irreversible aggregation detected by the Kratky plot. The temperature was 10 °C. Protein concentration was 16.3 mg/mL. From the top: 0.1, 50, 100, 150, 200, 150, 100, 50, and 0.1 MPa. Each line has been shifted so it can be clearly seen. LDH structure at 200 MPa at 25 °C. (c) Same plot as in (a), magnified in a small *S* region. From the top: 0.1, 50, 100, 150, and 200 MPa. (d) Same plot as in (b), magnified in a small *S* region. From the top: 200, 150, 100, 50, and 0.1 MPa.

observed in solution at atmospheric pressure (Table 1). The extrapolation to infinite-dilute solution was not done for high-pressure measurements, and therefore direct comparison of apparent R_g values with extrapolated data should be avoided. The displacement of subunits, however, should be detectable from apparent R_g before and after the compression cycle because the concentration dependency of R_g was small at atmospheric pressure. Since the recovery of activity is usually incomplete for 1000 min (*7*), R_g after the compression and decompression cycle should reflect mostly that of drifted LDH. The difference was very small: 34.3 ± 0.1 and 34.1 ± 0.1 Å for native and drifted LDH, respectively. We could not detect subunit displacement after reassociation.

Tertiary Structure Change in the Compression−Decompression Cycle. The equilibrium shift and packing of protein molecules were more pronounced in the Kratky plot ($S^2I(S)$ vs S plot, Figure 2). In the process of denaturation of small proteins such as staphylococcal nuclease, the height of the primary peak decreases as denaturation proceeds, and this is correlated with the loss of the secondary structure (*29*). The arrows in Figure 2c indicate the primary peaks of atmospheric pressure at 0.0083 Å^{-1} and of 200 MPa at 0.01 Å^{-1}. The position of the primary peak is a function of size, and therefore a side peak will appear in a multicomponent system. The shift of the primary peak to a wider S corresponds to a decrease in the size of the particle. In Figure 2c,d, the primary peak of transient pressure lies in one of

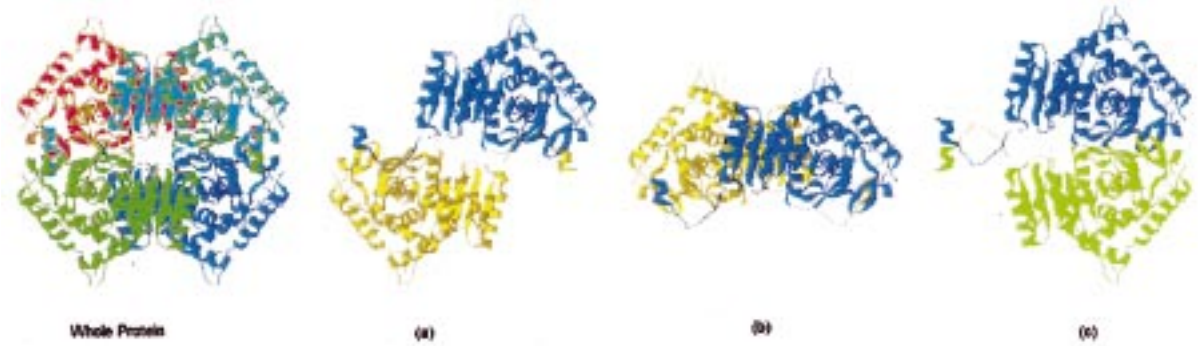

FIGURE 3: Combination of subunit orientations in LDH. From left to right: whole protein, model a, model b, and model c. Crystallographic coordinates are used from 6LDH (Protein Data Bank) (*28*). Colors show differences in the chain. The figure was produced using the RasMol2 program (*36*).

two positions, which indicates that the scattering curve is a mixture of only tetramer and dimer particles, i.e., two-state transition (*30*). If an intermediate state exists, a side maximum appears in the primary peak.

In Figure 2a, at ambient pressure, several peaks appear in 0.02−0.1 Å^{-1}, which is characteristic of the case of a multisubunit protein. This is due to the interference function of subunits (*31*). On decompression, the recovery of the interference function also showed a hysteresis effect in parallel with the change in R_g or $I(0)/C$.

Pressure-Induced Aggregation. Further application of high pressure to a dissociated dimer induced aggregation. Precipitation was observed at both 10 and 25 °C when pressures of more than 200 and 120 MPa were applied to LDH at 10 and 25 °C, respectively. In the state of precipitation, within a small *S* range, the scattering profile is greatly affected by the interparticle effect, and therefore determination of R_g was impossible. In a medium *S* range, however, the contribution of the interparticle effect becomes small, and no perturbations are expected unless the particles are stacked in a certain orientation (*21*). Even if anisotropy exists, a peak or interference corresponding to the correlation length would appear in SAXS profiles, which is not the case here. Figure 2b shows the formation process of aggregation by applying further pressure to LDH (16.3 mg/mL at 10 °C). Below 150 MPa, LDH dissociates into dimer as seen in Figure 2a. At 200 MPa, the first peak becomes flattened, which indicates the loss of bulk structure (*32*). The inner part of the Kratky plot during the release of pressure was plotted in Figure 2d. The small peak at 0.0072 Å^{-1}, which appeared at smaller *S* than that of native LDH, indicates that the loss of bulk structure accompanies the formation of aggregation. During decompression the height of the primary peak increased, and the equilibrium shifted to a stable large aggregation in which the bulk structure is formed. The peak position of aggregation at 0.0062 Å^{-1} was maintained during decompression, suggesting that the size of aggregation was constant. The subunit structure of irreversible aggregation is completely lost because no subunit interference is seen at medium angles.

From these results, we propose the following scheme in the case of precipitation:

$$\text{native tetramer} \leftrightarrow 2(\text{modified dimer}) \xrightarrow{\{\text{over pressure}\}} \text{unfolded aggregation} \Rightarrow \text{folded aggregation}$$

$$\xrightarrow{\{\text{reduction of pressure}\}}$$

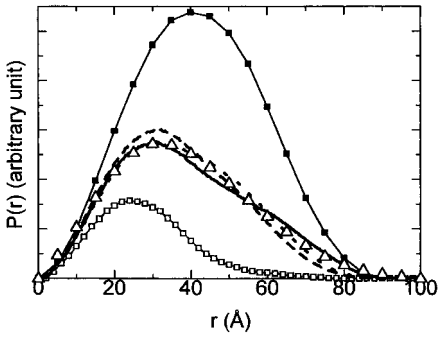

FIGURE 4: Characterization of model structures by SAXS. $P(r)$ function of model structures and experimental data at 200 MPa. $P(r)$ functions of model structures: LDH whole molecule (solid squares and line), model a (solid line), model b (broken line), model c (dotted line), LDH monomer (open squares and line), and experimental data at 200 MPa (open triangles). $P(r)$ of experimental data was scaled so as to fit model $P(r)$'s.

Subunit Orientation in the LDH Dimer. As shown in Figure 1, LDH dissociated into dimer at 200 MPa, 25 °C. In Figure 2a no conspicuous peaks arising from the tetramer were seen. The contribution of scattering from the tetramer is small. We therefore used the SAXS pattern at 200 MPa in the analysis of the LDH dimer. To determine the subunit orientation, we introduced noncrystallographic symmetry in the LDH dimer. If this assumption is invalid, no interference can be seen in the medium *S* region, which is common for most oligomeric proteins without symmetry or distinct shape. In the analysis of the medium *S* region, it is possible to determine the difference between a given structure and a solution structure, although it is difficult to determine the structure without additional information. Since apo-LDH has four subunits with 422 noncrystallographic symmetry (*28*), the combination of subunit orientation of the dimer out of four subunits is only three, as shown in Figure 3. It is natural to classify subunit orientation of the initial intermediate into these three candidates.

The $P(r)$ function in Figure 4 indicates that LDH at 200 MPa dissociated into dimers and that the molecular dimensions in the solution are not so deviated from the model dimer structures shown in Figure 3. It is very difficult, however, to select one orientation on the basis of Figure 4. This is because the contribution of interference at around a few nanometers, where a difference is supposed to exist, is several hundredths of the forward scattering intensity. While in reciprocal space, *S*, the form factor decreases rapidly as *S* increases; the interference originating from subunit orienta-

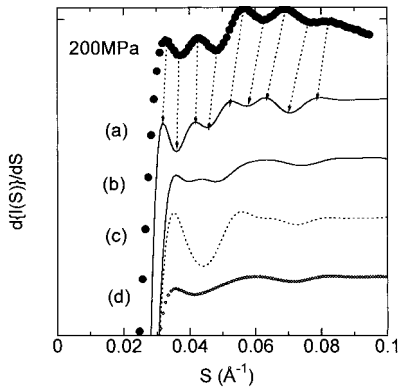

FIGURE 5: First derivative of $I(S)$. From the top: experimental data at 200 MPa (dotted line), model a, model b, and model c. Open circles represent monomer d. Curves have been shifted so they can be clearly seen. Dashed array shows the correspondence of peaks and drops to model data.

tion becomes more conspicuous than that in real space. To clarify the difference in the medium S region between candidate structures and the solution structure obtained experimentally, we took the first derivative of $I(S)$, $dI(S)/dS$. The procedure exaggerates peak positions that appear in medium S, but their height information will be lost. In Figure 5, it can be seen that the scattering patterns of the three candidates are very different. The experimental data have five peaks, showing that a dissociated dimer has a rigid tertiary structure. If this were not the case, less peaks would be expected because of the collapse of the core structure and, consequently, the loss of spatial interference like that observed in a molten globule state of a monomeric protein (*30*). This was very different from Arc repressor: when its dimer molecule becomes dissociated, the monomer takes on a molten globule structure (*33*).

The existence of five peaks is a very important clue to subunit orientation, because a combination of subunit orientations satisfying this pattern would be very limited. Among the three candidates shown in Figure 3, neither model b nor c has any fine structures in reciprocal space. Model a has the same number of peaks as that of the experimental data. The positions of the five peaks are different from those of the experimental data, but this is not important in considering orientation because peak positions are more dependent on the separation of two subunits. In Figure 5, experimental positions are shifted to larger S, which reflects the shortening of the separation in solution. This is consistent with the observation that R_g at 200 MPa is smaller than R_g of model a (Table 2). The solution structure, therefore, maintains an orientation similar to that of model a, with a shortened distance of two subunits. It is very interesting for LDH to choose the model a subunit configuration rather than other possibilities.

DISCUSSION

Contrast Effect by Pressure. In using forward scattering in high-pressure SAXS, the contrast effect should always be kept in mind, as the scattering phenomena comes from the difference in electron density between protein and bulk water or, more strictly, the excess electron density of a scattering particle with its associated hydration shell and bulk water. The isothermal compressibility of protein (about 10 $\times$ 10^{12} cm^2/dyn) is much smaller than that of water (45 $\times$ 10^{12} cm^2/dyn) (*34*), and therefore the excess electron density of the protein and its associated hydration shell decreases with increases in pressure. The change in contrast due to pressure particularly affects the forward scattering. $I(0)$ is proportional to the square product of mean excess electron density $\Delta\rho$ and volume V.

$$I(0) \propto (\Delta\rho V)^2$$

We measured the scattering change of lysozyme by sucrose contrast at atmospheric pressure as well as by high-pressure experiments in order to estimate the contrast effect. In the case of lysozyme, $I(0)$ decreased upon compression by 9% after being corrected for the absorption effect (*16*). This decrease includes both the decreases in $\Delta\rho$ and V. A change in contrast always accompanies a change in R_g (*35*). If the decrease in $I(0)$ comes only from contrast $\Delta\rho$, the 9% decrease in $I(0)$ corresponds to an electron density difference in 0.006 e/Å^3, estimated from a comparison with the decrease in $I(0)$ of contrast variation experiments. In this range of contrast, the change in R_g is so small that we can interpret hydrodynamic parameters under pressure as being practically the same as those at ambient pressure.

Apparent Violation of Le Chatlier's Principle of Pressure-Induced Dissociation of LDH. When LDH dissociates into dimer molecules, the initial stage involves the choice of subunit orientations out of three possibilities. To clarify the physical character of this process, R_g, Voronoi volume and surface area of three models are summarized in Table 2. First of all, it should be noted that model a, which is the most plausible orientation from SAXS, has neither the smallest volume nor the smallest surface area. It is model b that has the most compact structure in terms of R_g. If the dissociation pathway always follows the path to minimize a system volume, subunit orientation would be like model b. It is very difficult to give a clear answer as to why the dissociation did not take model b orientation. If one looks at Figure 3, model a has the most space between two subunits among the three possibilities, which consequently facilitates further compaction by shortening the distance between two subunits from the model a structure. The shortening of subunit distance is rationalized if Le Chatlier's principle is considered: the final volume of a system should decrease under pressure. The solution structure under pressure should need further structural change after choosing subunit orientation; otherwise, the total volume of dissociated products with a hydration shell would be larger than the initial volume of an oligomer particle in Table 2. This speculation is also consistent with the fact that radii of gyration of models were all larger than that of a dissociated product. The dissociation pathway picture seems to be as follows: by applying pressure, LDH dissociates into dimers so as to keep a subunit orientation as in model a; then with maintaining this orientation, the distance between two subunits shrinks by several angstroms without collapse of the structural core of each subunit.

Role of Aggregations on the Hysteresis Effect. When the aggregation stage is not too high, monomer aggregates can be restored to native structure under subdenaturing concentrations of urea (*11*). If the tetramerization reaction upon decompression includes dimer-to-tetramer as well as mono-

mer aggregation to tetramer, the observed hysteresis effect could be related to a fraction of the pressure of the unfolding species, which might be partially aggregated. SAXS data did not indicate an active role of aggregation in observed hysteresis. For one thing, the amount of aggregation here is very small. If any, it could be obvious in upperward curvature of the Guinier plot since scattering of aggregation is more intense than the native molecule. Second, the coexistence of unfolded aggregates affects the tail region of the Kratky plot as well as its primary peak position where a side maximum appears at a smaller S region, neither of which was observed. We note that the aggregation observed in this study, however, seems very irreversible and cooperative in its existence; the size did not change upon release of pressure, and there was no indication of the presence of a dissociated dimer or monomer when aggregation was formed. The crystal structure of an LDH subunit shows that the extended loop of its N-terminus interdigitates with each other to form a dimer as the smallest structural unit (*27*, *28*). An isolated monomer without a large modification of structure is therefore very unlikely, which is consistent with volume evaluation based on Le Chatlier's principle (Table 2). The subdenaturing concentration of urea seems to play an important role in keeping the aggregation stage reversible to native structure.

Heterogeneity of LDH and Lack of Concentration Dependence of Critical Pressure. Dissociation phenomena usually depend on protein concentration; however, SAXS results did not show a clear concentration dependence of critical pressure. When the equilibrium is a typical stochastic equilibrium in which all particles are indistinguishable with regard to the rates of association and dissociation, critical pressure follows the law of mass action. Such a lack of concentration dependence of critical pressure has been rationalized in terms of a heterogeneous distribution of free energy among the tetramer population (4). According to this scheme, at any pressure p, tetramers with free energy ΔG_i that obey the relation $\Delta G_i < p\Delta V_i$ will dissociate, whereas the remainder will stay unsplit. An alternative model that can account for a lack of concentration dependence is "kinetic control", where particle tetramers have such a wide distribution of activation barriers toward dissociation that a true dynamic equilibrium is never reached and critical pressure represents the fraction of tetramers whose dissociation rate constant is shorter than the experimental duration (*10*). In comparison with the above two models, SAXS results disfavor the heterogeneity of tetramers. If that is the case, the interference function of drifted LDH (Figure 2 or 5) will be more flattened. R_g of drifted LDH might differ from the native structure, which was not the case. The structure of a dissociated dimer, which takes a certain subunit orientation with shrinking distance, might have different steric activation barriers. Another point is that when the critical pressure is independent of concentration, reassociation of subunits must be inhibited. The SAXS model of a dissociated dimer suggests the compaction of subunit distance, which drastically reduces the subunit affinity.

In conclusion, R_g and $I(0)/C$ show a shift in equilibria. Together with the $P(r)$ function, dissociated products are shown to be dimers in which the core structure is retained. The subunit orientation is thought to be based on the interference of subunits that appear in a medium-angle region, whose subunit distance seems to be shortened. The model structure accounts for the apparent independence of concentration on critical pressure. SAXS results disfavor the conformational drift theory, though they cannot prove the role of reversible aggregation to the hysteresis effect.

ACKNOWLEDGMENT

The encouragement and support of Prof. Tatzuo Ueki (RIKEN), Prof. Yoshihiro Taniguchi (Ritsumeikan University), Prof. Tetsutaro Iizuka (RIKEN), and Prof. Yorinao Inoue (RIKEN) are greatly appreciated. We are grateful to Dr. Katsumi Kobayashi (PF) for help in maintaining the beamline. We thank Mr. Hideto Isogai and Mr. Masanori Matsumoto, graduate students of Ritsumeikan university, for operating the high-pressure pump.

REFERENCES

1. Jaenicke, R. (1981) *Annu. Rev. Biophys. Bioeng. 10*, 195−203.
2. Jaenicke, R. (1983) *Naturwissenschaften 70*, 332−341.
3. Jaenicke, R. (1987) in *Current perspectives in high-pressure biology* (Jannasch, H. M., et al., Eds.) pp 257−272, Academic Press, London.
4. Silvia, J. L., and Weber, G. (1993) *Annu. Rev. Phys. Chem. 44*, 89−113.
5. Mozhaev, V. V., Heremans, K., Frank, J., Masson, P., and Balny, C. (1996) *Proteins 24*, 81−91.
6. Gross, M., and Jearnicke, R. (1994) *Eur. J. Biochem. 221*, 617−630.
7. King, L., and Weber, G. (1986) *Biochemistry 25*, 3632−3637.
8. King, L., and Weber, G. (1986) *Biochemistry 25*, 3637−3640.
9. Cioni, P., and Strambini, G. B. (1996) *J. Mol. Biol. 263*, 789−799.
10. Cioni, P., and Strambini, G. B. (1997) *Biochemistry 36*, 8586−8593.
11. Gorovits, B. M., and Horowitz, P. M. (1998) *Biochemistry 37*, 6132−6135.
12. Fujisawa, T., Inoko, Y., and Ueki, T. (1993) *Biophysics 33* (Suppl.), S97.
13. Lorenzen, M., and Fiedler, S. (1997) *Biophysics*, 139−142.
14. Kleppinger, R., Goossens, K., Hermans, K., and Lorenzen, M. (1997) in *High-Pressure Research in the Biotechnology* (Hermans, K., Ed.) pp 135−138, Leuven University Press, Leuven.
15. Panick, G., Malessa, R., Winter, R., Rapp, G., Frye, K. J., and Royer, C. A. (1998) *J. Mol. Biol. 275*, 389−402.
16. Kato, M., and Fujisawa, T. (1998) *J. Synchrotron Radiat. 5*, 1282−1286.
17. Ueki, T., Hiragi, Y., Kataoka, M., Inoko, Y., Amemiya, Y., Izumi, Y., Tagawa, H., and Muroga, Y. (1985) *Biophys. Chem. 23*, 115−124.
18. Fujisawa, T., Uruga, T., Yamaizumi, Z., Inoko, Y., Nishimura, S., and Ueki, T. (1994) *J. Biochem. 115*, 875−880.
19. Moore, P. B. (1980) *J. Appl. Crystallogr. 13*, 168−175.
20. Svergun, D. I., Semenyuk, A. V., and Feigin, L. A. (1988) *Acta Crystallogr., Sect. A 44*, 244−250.
21. Guinier, A., and Fournet, G. (1955) in *Small-Angle Scattering of X-rays*, John Wiley, New York.
22. Svergun, D., Baberato, C., and Koch, M. H. J. (1995) *J. Appl. Crystallogr. 28*, 768−773.
23. Harpaz, Y., Gerstein, M., and Cothia, C. (1994) *Structure 2*, 641−649.
24. Gerstein, M., Tsai, J., and Levitt, M. (1995) *J. Mol. Biol. 249*, 955−966.
25. Gekko, K., and Timasheff, S. N. (1981) *Biochemisty 20*, 4667−4676.
26. Monod, J. (1966) *Science 154*, 475−483.
27. Grau, U. M., Trommer, W. E., and Rossmann, M. G. (1981) *J. Mol. Biol. 151*, 289−307.

28. Abad-Zapatero, C., Griffith, J. P., Sussman, J. L., and Rossmann, M. G. (1987) *J. Mol. Biol. 198*, 445−467.
29. Kataoka, M., Nishii, I., Fujisawa, T., Ueki, T., Tokunaga, F., and Goto, Y. (1995) *J. Mol. Biol. 249*, 215−228.
30. Kataoka, M., Flanagan, J. M., Tokunaga, F., and Engelman, D. M. (1994) in *Synchrotron Radiation in the Biosciences* (Chance, B., Deisenhofer, J., Ebashi, S., Goodhead, D. T., Helliwell, J. R., Huxley, H. E., Iizuka, T., Kirz, J., Mitsui, T., Rubenstein, E., Sakabe, N., Sasaki, T., Schmahl, G., Stuhrmann, H. B., Wurtrich, K., and Zaccai, G., Eds.) pp 187−194, Oxford University Press, Oxford.
31. Ueki, T., Inoko, Y., Kataoka, M., Amemiya, Y., and Hiragi, Y. (1986) *J. Biochem. 99*, 1127−1136.
32. Flanagan, J. F., Kataoka, M., Fujisawa, T., and Engelman, D. (1993) *Biochemistry 32*, 10359−10370.
33. Peng, X., Jonas, J., and Silvia, J. (1993) *Proc. Natl. Acad. Sci. U.S.A. 90*, 1776−1780.
34. Gekko, K., and Hasegawa, Y. (1986) *Biochemistry 25*, 6563−6571.
35. Feigin, L. A., and Svergun, D. I. (1987) in *Structure Analysis by Small-Angle X-ray and Neutron Scattering*, Plenum Press, New York.
36. Sayle, R. A., and Milner-White, E. J. (1995) *Trends Biochem. Sci. 20*, 374.

BI982558D